Journal of Nanoscience and Nanotechnology
Vol. 13, 6254–6258, 2013

Monte Carlo Study on the Self-Assembly of Nanoparticles Into a Nanorod Structure

Mohammad A. Matin[1], Hyojeong Kim[1], Joyanta K. Saha[1], Zhengqing Zhang[1], Jinkwon Kim[2], and Joonkyung Jang[1,*]

[1] *Department of Nanomaterials Engineering, Pusan National University, Miryang 627-706, Republic of Korea*
[2] *Department of Chemistry, Kongju National University, Kongju 314-701, Republic of Korea*

It is well known that semiconductor nanoparticles (NPs) can assemble into a range of low dimensional structures, such as nanowires, nanorods and nanosheets. In this study, we investigate the self-assembly of CdTe NPs by using Monte Carlo simulation. Using a simple model for the anisotropic interaction of NPs, the present Monte Carlo simulation demonstrated that NPs with large dipole moments assemble spontaneously into a nanorod even if the short range interactions among NPs is isotropic. Interestingly, we found that the present nanorod grew by forming a transient structure which looks similar to a double ring. For NPs similar to CdTe, the dipole–dipole interaction had a dominant effect over van der Waals attractions and steric repulsion on the final structure of the NP aggregates. The simulated rods are similar to those observed in the experimental self-assembly of CdTe NPs. The NPs with relatively small electric dipole moments aggregated into more or less isotropic structures.

Keywords: Nanoparticle, Self Assembly, Low Dimensional Structure, Dipole–Dipole Interaction, van der Waals Interaction, Nanorod.

1. INTRODUCTION

The strong size- and shape-dependent photonic and electronic properties[1] of semiconductor nanoparticles (NPs) highlight their potential as the constituting material for nanoscale opto-electronic devices,[2–4] photovoltaic devices,[5,6] optical amplifier media,[7,8] biolabeling,[9–11] and *in vivo* imaging and diagnostics for living cells.[12] NPs can assemble spontaneously into low dimensional structures, such as quantum dots,[13] rods,[14,15] wires,[16,17] cubes,[18] nanoribbons,[19] tetrapods,[20] and triangular prisms[21] in isotropic solution. On the other hand, little is known about the molecular mechanisms of this rather surprising self assembly of NPs.

From a fundamental point of view, it is important to understand self-assembled nanostructures in terms of the pairwise interaction of individual NPs. Experiments have shown that the dipole–dipole interactions among NPs is the main driving force in NP self organization.[22,23] Group II–VI semiconductor NPs with both hexagonal (i.e., wurtzite) and cubic (i.e., zinc blende) crystal structures were found experimentally to possess significant dipole moments.[24–26] In addition to the dipole–dipole interaction, the van der Waals interaction and hydrogen bonding between stabilizers are also important in self-assembled structures.

In addition to experimental efforts, computer simulations can provide detailed insights into the self assembly of NPs, which is difficult to achieve by other means. Indeed, the assembly of polymer-tethered nanorods has been simulated extensively.[27–30] The Glotzer group carried out Monte Carlo (MC) simulations on the self assembly of cubic NPs.[31] Conventionally, the anisotropic structure of self assembly was simulated by building in an anisotropic short-range interparticle potential. For example, the Glotzer group reproduced the experimental nanosheet structure using an anisotropic short range interaction potential in their simulation, which drives the self assembly toward the desired anisotropic structure.[32] The present paper reports that a rod-like structure of the NP assembly can be obtained through the dipole–dipole interaction, even with an isotropic short-ranged interaction between NPs (which has no preference for an anisotropic assembly). The nanorod grows by forming an intriguing transient structure that has the appearance of a double ring.

*Author to whom correspondence should be addressed.

 1533-4880/2013/13/6254/005 doi:10.1166/jnn.2013.7684

2. MODEL AND SIMULATION METHOD

In the present MC simulation, each NP was modeled as a dipolar sphere with a radius of 1.5 nm. The electric dipole moment of NP was varied from 100 to 500 D. The interaction between the electric dipoles of the *i*th and *j*th NPs was described by the potential function reported by Phillies,[33]

$$U_{ij}^{\text{dipole}} = \frac{\mu_i \mu_j}{4\pi\varepsilon_o \varepsilon r_{ij}^3}\{\cos\theta_i \cos\theta_j [2+kr_{ij}+(kr_{ij})^2] + \sin\theta_i \sin\theta_j \cos(\phi_i-\phi_j)[1+kr_{ij}]\} e^{-kr_{ij}} C_1^2 \quad (1)$$

where r_{ij} is the center-to-center distance between two NPs, and θ_i is the angle of the dipole vector with respect to the vector connecting the centers of the particles. ϕ_i is the dihedral angle describing the relative orientation of the dipoles. μ_i is the dipole moment of the *i*th particle. $1/k$ is the Debye screening length set to the diameter of NP, 3 nm. ε_0 and ε are the permittivities of the vacuum and solvent (water), respectively. C_1 in Eq. (1) is given by the following:

$$C_1 = \frac{3e^{ka}}{[2+2ka+(ka)^2+(1+ka)/\varepsilon_r]} \quad (2)$$

where ε_r is the ratio of the dielectric constants of NP and solvent, and a is the radius of NP (1.5 nm). The dispersion interaction between NPs can be expressed as[34]

$$U_{ij}^{vdw}(r_{ij}) = -\frac{A_{121}}{12}\left\{\frac{4a^2}{r_{ij}^2-4a^2}+\frac{4a^2}{r_{ij}^2}+2\ln\left[\frac{r_{ij}^2-4a^2}{r_{ij}^2}\right]\right\} \quad (3)$$

where A_{121} is the Hamaker constant of NP. A_{121} was set to be the same value as that reported for CdS particles interacting in water, $A_{121} = 4.85 \times 10^{-20}$ J.[35] The short-range steric repulsion between NPs in the presence of organic stabilizer molecules (thioglycolic acid, for example) on the NP surface was also considered. This interaction was modeled using the de Gennes expression,[36]

$$U_{ij}^{\text{steric}}(r_{ij}) = \frac{100a\delta_{\text{SAM}}^2}{(r_{ij}-2a)\pi\sigma_{\text{thiol}}^3} k_B T \exp\left(\frac{-\pi(r_{ij}-2a)}{\delta_{\text{SAM}}}\right) \quad (4)$$

where δ_{SAM} is the brush thickness of the stabilizer on NP, which was taken to be the length of thioglycolic acid (here the literature value, 5 Å, was taken.[32, 37]). σ_{thiol} is the separation distance between stabilizers on the NP surface, which was set to the literature value, 4.3 Å.[38] Note the present van der Waals potential, Eq. (3), does not contain the repulsion between nanoparticles. Therefore, the short-ranged steric interaction, Eq. (4), is needed to prevent collapse of nanoparticles into one. This streric interaction is also needed to take into account the presence of stabilizers on nanoparticles.

Using the potential functions above, Eqs. (1)–(4), a constant number, volume, and temperature (NVT) Monte Carlo simulation was run for 100 NPs scattered randomly in a cubic simulation box with a length of 400 Å. The temperature was fixed to 100 K to facilitate particle aggregation. Periodic boundary conditions were imposed. A MC step was defined as a trial move to translate the particle or rotate the dipole of the particle. 30 million MC

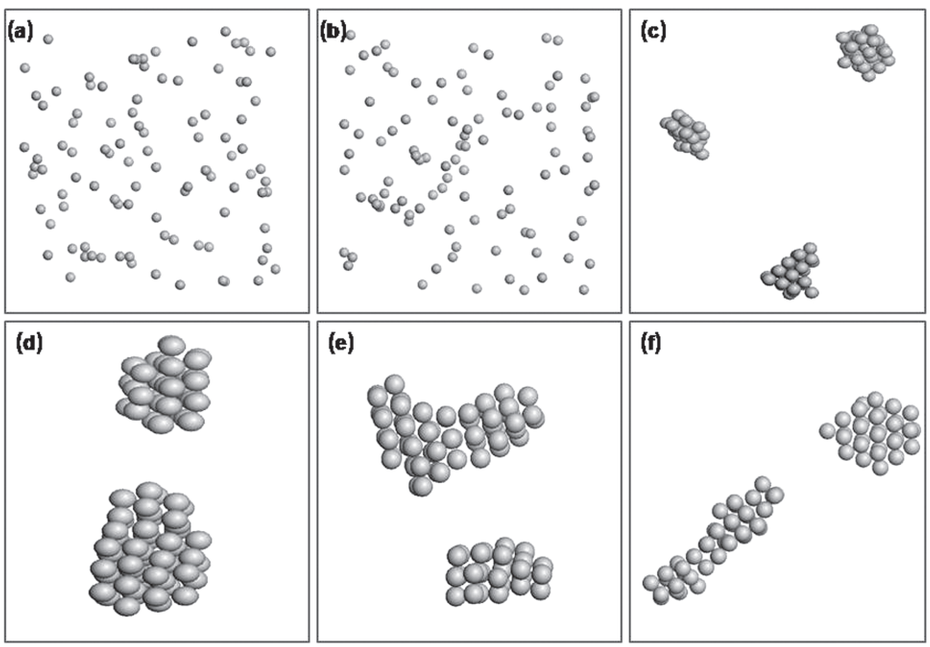

Fig. 1. Final snapshots of a Monte Carlo simulation for nanoparticles with various electric dipole moments, (a) 100 D, (b) 200 D, (c) 250 D, (d) 300 D, (e) 400 D, and (f) 500 D.

RESEARCH ARTICLE

steps were run and that the total energy of system converged to a constant as the NPs self assembled.

3. RESULTS AND DISCUSSION

This study first examined how the dipole moment of NP affects the self-assembly of NPs. As shown in Figure 1, NPs with relatively small dipole moments ((a) and (b), NPs with the dipole moments of 100 and 200 D, respectively) do not aggregate, except for several unstable (with respect to thermal fluctuation) clusters comprised of 2 to 4 NPs. Slightly anisotropic aggregation of NPs was observed when the dipole moment of the NPs was increased to 250 and 300 D, as shown in Figures 1(c) and (d), respectively. For NPs with a 250 D dipole moment, the final aggregation, on average, ranged from 4 to 5 NPs in length and 2 to 3 NPs in thickness. These aggregations gradually grew through the merging of small clusters made from 2 to 5 NPs, which formed rapidly as the simulation began (within 3×10^5 MC steps). With increasing dipole moment of NPs from 250 to 300 D ((c) to (d)), small clusters of 5 to 6 NPs formed at the early stages of the simulation. As the simulation progressed, these small clusters coalesced and elongated in a single direction. The length of aggregation ranged from 5 to 7 NPs and the thickness ranged from 3 to 4 NPs. A rod-like feature was evident in the final aggregation of NPs with the two strongest dipole moments ((e) and (f)). The NPs first made small isotropic aggregates, which then assembled into a rod-like aggregation. For NPs with a dipole moment of 400 D, the nanorod ranged from 5 to 7 NPs in length and 2 to 3 NPs in thickness. For the NPs with the largest dipole (500 D, (f)), a rod-like shape was clearly observed in the larger aggregate of two. The larger nanorod was 10 NPs in length and 2 to 3 NPs in thickness. To the author's knowledge, the growth of a nanorod has not been reported in previous computer simulations. Unlike previous studies,[39, 40] the present model did not build in any anisotropy in the short-ranged interaction (van der Waals and steric interactions) or in the shape of NPs, which facilitates anisotropic aggregation in the simulation.

The nanorod shown in Figure 1(f) grew by forming an interesting transient structure. As the simulation proceeded, the NPs formed double ring structures, as shown in Figure 2(b). Several single rings were also observed (not drawn here). The dipole moments of the NPs (drawn as arrows) in the double ring were oriented head-to-tail. These ring structures grew in size by merging with other NPs. At the same time, the ring became squeezed and

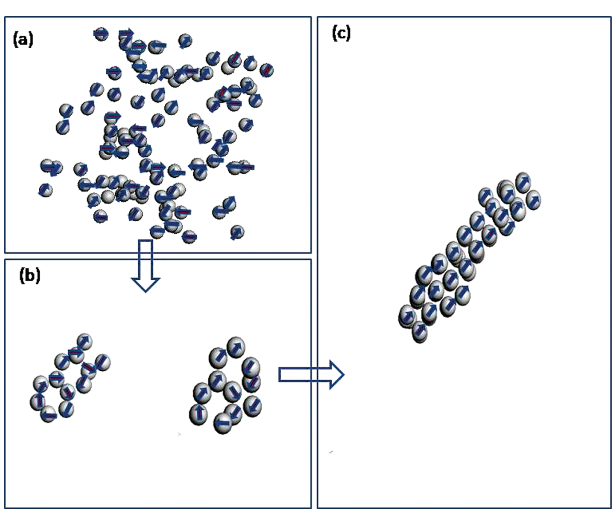

Fig. 2. Transient double-ring structure in the formation of a nanorod starting from randomly dispersed nanoparticles with a dipole moment of 500 D. Shown are dispersed nanoparticles at the early stage of the simulation (a), transient double ring structures (b), and final nanorod structure (c). The arrows represent the direction of the electric dipole moment of each nanoparticle.

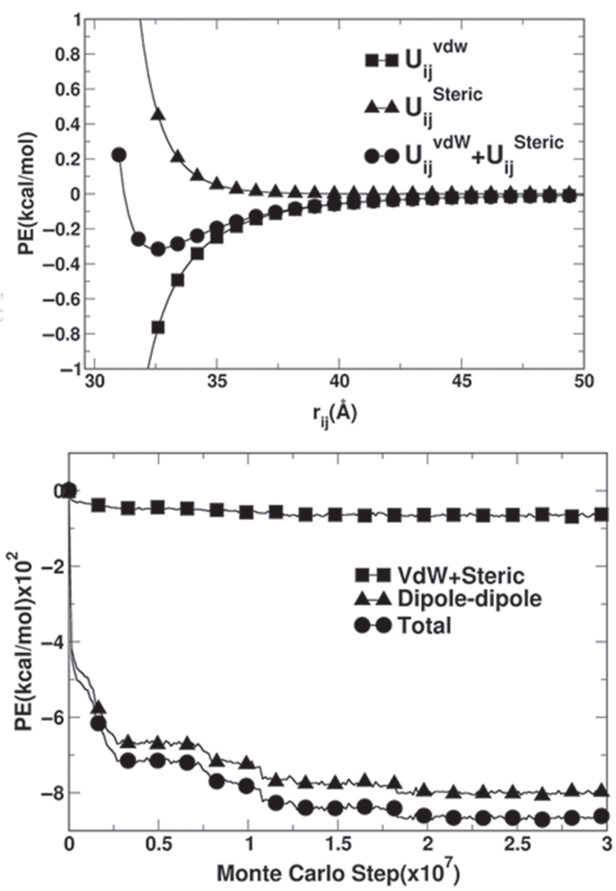

Fig. 3. Energetics behind the formation of a nanorod (500 D and 100 NPs). The pairwise interparticle potential energy versus the center-to-center distance between NPs, r_{ij}, (line with circles) is projected into the van der Waals (line with squares) and the steric interaction (line with triangles) potential functions (top). The total potential energy of system versus Monte Carlo step (bottom). The total potential energy (drawn as a line with circles), the potential energy due to the dipole–dipole interaction (line with triangles), and the potential energy from the sum of the van der Waals interaction and steric interaction (line with squares) potential functions are plotted.

the hole of the ring vanished. In this way, the aggregate lengthens in one direction to give a rod-like structure, as shown in Figure 2(c). The electric dipoles orient head-to-tail along the long axis of the nanorod but they are stacked parallel along a direction perpendicular to the long axis.

This study examined the energetics behind the formation of nanorods. The top of Figure 3 is the pairwise interaction potential function between NPs with dipole moments of 500 D. The total interparticle potential in this case is dominated by the dipole–dipole interaction (here, the two dipoles are assumed to align head to tail). The sum of the van der Waals attractions and short ranged steric repulsion has a potential well depth of approximately $(1/2)k_B\mathrm{T}$, which is insufficient to stabilize NP aggregation under ambient conditions. The bottom of Figure 3 shows the total potential energy versus MC step for 100 NPs (with dipole moments of 500 D) that were initially randomly scattered. The total potential energy decreased rapidly as the simulation started, and then decreased gradually, converging to a constant within 2×10^7 MC steps. Several plateaus were observed in the energy versus MC step curve, which correspond to intermediate aggregates before the formation of the final aggregation. Here too, the dipole–dipole attraction had a dominant effect over the van der Waals interaction for the entire period of the simulation.

It is possible that the present MC sampling of the configuration space is insufficient, and, as a result, the nanorod structure shown in Figure 2(c) might further grow. For more effiecent sampling of the configuration space, MC moves such as the cluster moves[41] might be needed.

4. CONCLUSIONS

Using a simplistic model for the anisotropic interaction of semiconductor NPs, the present Monte Carlo simulation demonstrated that NPs with large dipole moments (500 D) assemble spontaneously into a nanorod even if the short range interactions among NPs is isotropic. The NPs with relatively small electric dipole moments aggregated into more or less isotropic structures or small clusters[41] made from 3 or 4 NPs. For NPs similar to CdTe, the dipole–dipole interaction had a dominant effect over van der Waals attractions and steric repulsion on the final structure of the NP aggregates. The nanorod grew by rapidly, forming small clusters of 3 to 4 NPs and producing transient double ring structures.

Acknowledgments: This study was supported by the Korean Research Foundation (KRF) grant funded by the Korea government (MEST) (Nos. 2012-047626 and 2011-0003078).

References and Notes

1. A. P. Alivisatos, *Science* 271, 933 (**1996**).
2. H. Mattoussi, L. H. Radzilowski, B. O. Dabbousi, E. L. Thomas, M. G. Bawendi, and M. F. Rubner, *J. Appl. Phys.* 83, 7965 (**1998**).
3. M. C. Schlamp, P. Xiaogang, and A. P. Alivisatos, *J. Appl. Phys.* 82, 5837 (**1997**).
4. M. Gao, C. Lesser, S. Kirstein, H. Möhwald, A. L. Rogach, and H. Weller, *J. Appl. Phys.* 87, 2297 (**2000**).
5. K. Barnham, J. L. Marques, J. Hassard, and P. O'Brien, *Appl. Phys. Lett.* 76, 1197 (**2000**).
6. N. C. Greenham, P. Xiaogang, and A. P. Alivisatos, *Phys. Rev.* B 54, 17628 (**1996**).
7. M. T. Harrison, S. V. Kershaw, M. G. Burt, A. L. Rogach, A. Kornowski, A. Eychmüller, and H. Weller, *Pure Appl. Chem.* 72, 295 (**2000**).
8. S. V. Kershaw, M. Harrison, A. L. Rogach, and A. Kornowski, *IEEE J. Select. Topics Quantum Electron* 6, 534 (**2000**).
9. H. Mattoussi, J. M. Mauro, E. R. Goldman, G. P. Anderson, V. C. Sundar, F. V. Mikulec, and M. G. Bawendi, *J. Am. Chem. Soc.* 122, 12142 (**2000**).
10. M. Bruchez, Jr, M. Moronne, P. Gin, S. Weiss, and A. P. Alivisatos, *Science* 281, 2013 (**1998**).
11. W. C. W. Chan and S. Nie, *Science* 281, 2016 (**1998**).
12. X. Michalet, F. F. Pinaud, L. A. Bentolila, J. M. Tsay, S. Doose, J. J. Li, G. Sundaresan, A. M. Wu, S. S. Gambhir, and S. Weiss, *Science* 307, 538 (**2005**).
13. J. Li, Y. Jiang, D. Wu, W. Wang, J. Huang, C. Liu, B. Wang, and Z. J. Zhang, *J. Nanosci. Nanotechnol.* 12, 3806 (**2012**).
14. C. Pacholski, A. Kornowski, and H. Weller, *Angew. Chem. Int. Ed.* 41, 1188 (**2002**).
15. B. Joo, Y. Jun, B. K. Min, E. Koo, Y. R. Do, and S. J. Yoon, *J. Nanosci. Nanotechnol.* 12, 1638 (**2012**).
16. J. Y. Chang, J. J. Chang, B. Lo, S. H. Tzing, and Y. C. Ling, *Chem. Phys. Lett.* 379, 261 (**2003**).
17. S. Liu, C. Yang, W.-H. Zhang, and C. Li, *J. Nanosci. Nanotechnol.* 11, 11181 (**2011**).
18. D. Yu and V. W.-W. Yam, *J. Am. Chem. Soc.* 126, 13200 (**2004**).
19. S.-M. Park, W.-K. Kang, J. W. Kang, Y. K. Hong, and K.-S. Kim, *J. Nanosci. Nanotechnol.* 12, 4309 (**2012**).
20. L. Manna, E. C. Scher, and A. P. Alivisatos, *J. Am. Chem. Soc.* 122, 12700 (**2000**).
21. N. Malikova, I. P.-Santos, M. Schierhorn, N. A. Kotov, and L. M. L.-Marzán, *Langmuir* 18, 3694 (**2002**).
22. H. S. Park, A. Agarwal, N. A. Kotov, and O. D. Lavrentovich, *Langmuir* 24, 13833 (**2008**).
23. J. Y. Chang, H. Wu, H. Chen, Y. C. Ling, and W. Tan, *Chem. Commun.* 8, 1092 (**2005**).
24. E. Rabani, *J. Chem. Phys.* 115, 1493 (**2001**).
25. M. Shim and P. Guyot-Sionnest, *J. Chem. Phys.* 111, 6955 (**1999**).
26. S. A. Blanton, R. L. Leheny, M. A. Hines, and P. Guyot-Sionnest, *Phys. Rev. Lett.* 79, 865 (**1997**).
27. L. He, L. Zhang, Y. Ye, and H. Liang, *J. Phys. Chem. B* 114, 7189 (**2010**).
28. M. A. Horsch, Z. Zhang, and S. C. Glotzer, *Phys. Rev. Lett.* 95, 056105 (**2005**).
29. M. A. Horsch, Z. Zhang, and S. C. Glotzer, *Nano Lett.* 6, 2406 (**2006**).
30. T. D. Nguyen and S. C. Glotzer, *ACS Nano* 4, 2585 (**2010**).
31. X. Zhang, Z. Zhang, and S. C. Glotzer, *J. Phys. Chem. C* 111, 4132 (**2007**).
32. Z. Zhang, Z. Tang, N. A. Kotov, and S. C. Glotzer, *Nano Lett.* 7, 1670 (**2007**).

33. G. D. Phillies, *J. Chem. Phys.* 60, 2721 **(1974)**.
34. H. C. Hamaker, *Physica* (*Utrecht*) 4, 1058 **(1937)**.
35. I. D. Morrison and S. Ross, Colloidal Dispersions, Suspensions, Emalsions and Foams, Wiley-Interscience, New York **(2002)**.
36. A. Ulman, *J. Mater. Ed*. 11, 205 **(1989)**.
37. Z. Tang, B. Ozturk, Y. Wang, and N. A. Kotov, *J. Phys. Chem. B* 108, 6927 **(2004)**.
38. B. A. Korgel, S. Fullam, S. Connolly, and D. Fitzmaurice, *J. Phys. Chem. B* 102, 8379 **(1998)**.
39. A. Y. Sinyagin, A. Belov, Z. Tang, and N. A. Kotov, *J. Phys. Chem. B* 110, 7500 **(2006)**.
40. J. Richardi, *J. Chem. Phys*. 130, 044701 **(2009)**.
41. D. Frenkel and B. Smit, Understanding Molecular Simulation: From Algorithms to Applications, Academic Press, San Diego, U.S.A **(2002)**.

Received: 20 July 2012. Accepted: 20 December 2012.